

Expansion Planning for Renewable Integration in Power System of Regions with Very High Solar Irradiation

Musfer Alraddadi, Antonio J. Conejo, and Ricardo M. Lima

Abstract—In this paper, we address the long-term generation and transmission expansion planning for power systems of regions with very high solar irradiation. We target the power systems that currently rely mainly on thermal generators and that aim to adopt high shares of renewable sources. We propose a stochastic programming model with expansion alternatives including transmission lines, solar power plants (photovoltaic and concentrated solar), wind farms, energy storage, and flexible combined cycle gas turbines. The model represents the long-term uncertainty to characterize the demand growth, and the short-term uncertainty to characterize daily solar, wind, and demand patterns. We use the Saudi Arabian power system to illustrate the functioning of the proposed model for several cases with different renewable integration targets. The results show that a strong dependence on solar power for high shares of renewable sources requires high generation capacity and storage to meet the night demand.

Index Terms—Generation and transmission expansion planning, uncertainty, solar power, wind power.

NOMENCLATURE

A. Indices

δ	Scenario
b	Storage unit
d	Demand
j	Combined cycle gas turbine (CCGT)
l	Transmission line
n	Node
o	Day
$r(l)$	Receiving-end node of transmission line l
s	Solar unit

$s(l)$ Sending-end node of transmission line l

t Time period

w Wind unit

B. Sets

\mathcal{Q}_n^B Storage units located at node n

\mathcal{Q}_n^D Demands located at node n

\mathcal{Q}_n^J CCGTs located at node n

\mathcal{Q}^L Prospective transmission lines

\mathcal{Q}_n^S Solar units located at node n

\mathcal{Q}_n^W Wind units located at node n

\mathcal{Q}_r Reference nodes

C. Parameters

α_o Weight of day o

β_δ Probability of scenario δ

η_b Energy efficiency of storage unit b

σ_j The minimum power output coefficient of CCGT j

φ^{EA} Per unit factor regarding average renewable energy

φ^{EE} Per unit factor regarding renewable energy per scenario

φ^C Per unit factor regarding renewable power

B_l Susceptance of transmission line l

C_d^U Load-shedding cost of demand d

C_j^J Production cost of CCGT j

C_s^S Production cost of solar unit s

C_w^W Production cost of wind unit w

$\bar{E}_b^{B,\max}$ The maximum energy capacity that can be built of storage unit b

F_l^{\max} Capacity of transmission line l

$F_{\delta,s,o,t}^S$ Solar capacity factor of solar unit s in scenario δ at hour t of day o

$F_{\delta,w,o,t}^W$ Wind capacity factor of wind unit w in scenario δ at hour t of day o

I_b^B Annualized investment cost of storage unit b

$I^{G,\max}$ Investment budget for building gas, wind, solar, and storage units

I_j^J Annualized investment cost of CCGT j

Manuscript received: October 20, 2019; accepted: June 22, 2020. Date of CrossCheck: June 22, 2020. Date of online publication: September 15, 2020.

This article is distributed under the terms of the Creative Commons Attribution 4.0 International License (<http://creativecommons.org/licenses/by/4.0/>).

M. Alraddadi (corresponding author) is with the Department of Electrical and Computer Engineering, The Ohio State University, Columbus, OH 43210, USA (e-mail: Alraddadi.4@osu.edu).

A. J. Conejo is with the Department of Integrated Systems Engineering and the Department of Electrical and Computer Engineering, The Ohio State University, Columbus, OH 43210, USA (e-mail: conejonavarro.1@osu.edu).

R. Lima is with King Abdullah University of Science and Technology, Thuwal 23955-6900, Kingdom of Saudi Arabia (e-mail: ricardo.lima@kaust.edu.sa).

DOI: 10.35833/MPCE.2019.000112



I_l^N	Annualized investment cost of prospective transmission line l
$I^{L,\max}$	Investment budget for building transmission lines
I_s^S	Annualized investment cost of solar unit s
I_w^W	Annualized investment cost of wind unit w
M	Large enough positive constant
$p_b^{BP,\max}$	Charging capacity of storage unit b
$p_b^{BT,\max}$	Discharging capacity of storage unit b
$P_{\delta,d,t,o}^D$	Load of demand d in scenario δ at hour t of day o
$\bar{P}_j^{J,\max}$	The maximum capacity that can be built of CCGT j
$\bar{P}_s^{S,\max}$	The maximum capacity that can be built of solar unit s
$\bar{P}_w^{W,\max}$	The maximum capacity that can be built of wind unit w
R_j^D	Ramping-down limit of CCGT j
R_j^U	Ramping-up limit of CCGT j
<i>D. Binary Variables</i>	
x_l	Binary variable that is equal to 1 if prospective transmission line l is built and 0 otherwise
$y_{\delta,j,o,t}$	Binary variable that is equal to 1 if CCGT j is on-line in scenario δ at hour t of day o , and 0 otherwise
<i>E. Continuous Variables</i>	
$\theta_{\delta,n,o,t}$	Voltage angle at node n in scenario δ at hour t of day o
$E_b^{B,\max}$	Energy capacity of storage unit b
$E_{\delta,b,o,t}^B$	Energy in storage unit b in scenario δ at the beginning of hour t of day o
$F_{\delta,l,o,t}^L$	Power flow through transmission line l in scenario δ at hour t of day o
$p_{\delta,b,o,t}^{B,T}$	Discharging power from storage unit b in scenario δ at hour t of day o
$p_{\delta,b,o,t}^{B,P}$	Charging power to storage unit b in scenario δ at hour t of day o
$p_{\delta,d,o,t}^{D,U}$	Load shed of demand d in scenario δ at hour t of day o
$P_j^{J,\max}$	Capacity of CCGT j
$p_{\delta,j,o,t}^J$	Power produced by CCGT j in scenario δ at hour t of day o
$P_s^{S,\max}$	Capacity of solar unit s
$p_{\delta,s,o,t}^{S,\text{spill}}$	Spilled power of solar unit s in scenario δ at hour t of day o
$P_w^{W,\max}$	Capacity of wind unit w
$p_{\delta,w,o,t}^{W,\text{spill}}$	Spilled power of wind unit w in scenario δ at hour t of day o
$x_{\delta,j,o,t}$	Product of binary variable $y_{\delta,j,o,t}$ and continuous variable $P_j^{J,\max}$ in scenario δ at hour t of day o
$z_{\delta,j,o,t}$	Positive slack variable of CCGT j in scenario δ at hour t of day o
$P_{\delta,d,t,o}^D$	Load of demand d in scenario δ at hour t of day o

I. INTRODUCTION

IN this paper, we propose a generation and transmission expansion model motivated by an energy transition in regions with very high solar irradiation. These regions are strong candidates for a transition from a power system based on thermal generation to the one based on solar power. Examples of regions with very high solar irradiation include southwest USA, the Arabian Peninsula, north of Africa, Inner Mongolia and Tibet in China, north of Mexico, western and central Australia, western Pakistan, western South Africa, and north Chile. However, a number of challenges exist to incorporate solar power in power systems [1]. The aforementioned regions have a strong and widespread availability of solar resources, but integrating these resources requires technical and economic analyses of viable percentages of different technologies including energy storage. In addition, it is relevant to assess the operation complementarity of solar and other renewable sources. Overall, these analyses are relevant to support decision-makers on where and when to install renewable sources.

We propose a stochastic programming model to address the generation and transmission expansion planning that involves the selection of alternative generation plants, energy storage, and transmission lines to install. We adopt a green-field perspective for the generation plants, but not for the transmission lines. Planning new transmission lines is important to avoid congestions due to the integration of renewable sources, which is spatially conditioned by the locations of resources. We model both long- and short-term uncertainties. Long-term uncertainty pertains to demand growth patterns across the region of interest and it is represented using a number of scenarios. Short-term uncertainty refers to the daily variation of the electricity demand and the power production of solar and wind facilities and it is represented using a number of typical days. The objective of the model is to minimize total costs, and a number of case studies are considered with increasing renewable integration targets, from business as usual (BAU) to 100% renewable sources, and the outcome is analyzed in terms of generation mix, energy storage, investment costs, and operation costs.

Generation and transmission expansion planning models have been evolving to accommodate reliability targets, renewable generation plants, environmental concerns, and others. This planning problem can be analyzed and studied from multiple perspectives, depending on the objectives and context of the considered power system. The relevance to the society and the economy of this problem has originated a large number of works. Therefore, we limit our review to those related to our work, and refer the reader to [2]-[4] for comprehensive reviews on different perspectives. Reference [5] focuses on generation and transmission expansion planning, where wind power investments and associated transmission reinforcements are determined to minimize consumer payments. A relevant perspective in planning is the value of storage to facilitate the integration of renewable sources. In this regard, [6] discusses the benefits of energy storage systems to integrate weather-dependent renewable sources. Also, in [7], a number of case studies in renewable integration

are discussed in detail and relevant suggestions are made to achieve better integration of renewable sources in the USA. Regarding generation and transmission expansion, [8] proposes an integrated formulation that accounts for a probabilistic reliability criterion. Reference [9] focuses on the generation expansion problem considering the uncertainty in the load and wind power output and uses a two-stage stochastic programming formulation. The alternative renewable policy scenarios and their impact on CO₂ emissions are studied. Reference [10] focuses on long-term uncertainties such as carbon and fuel prices, demand, and renewable penetration at the European level. A power system involving multiple regions with transmission limits between regions is considered. A relevant topic in these models is the characterization of the short-term uncertainty of hourly wind and solar power output, and of the demand. Reference [11] proposes an optimization-based approach to select representative days, which shows that their approach decreases the computation resources required to solve generation expansion planning problems. Reference [12] focuses on the generation expansion problem for the integration of large amounts of wind, which proposes a multi-stage stochastic programming formulation where some decisions affect future uncertainties. Reference [13] proposes a generation expansion planning model with investments occurring at different years and involving various energy sources (wind, solar, coal, natural gas, and nuclear). A nested Benders decomposition algorithm is developed to address the computation challenges of large instances. However, long-term uncertainty and transmission constraints are not considered. Reference [14] describes a generation and transmission expansion planning model to support investment decisions to move to a fully renewable power system from a thermal dominated one. Reference [15] analyzes the impact of considering detailed unit commitment constraints on investment results related to generation capacity and energy storage, which shows that ignoring those constraints leads to building less storage in the system, but as expected, the complexity of the model increases substantially due to the number of binary variables introduced by the commitment of thermal units. As a final reference, we mention [16], a book regarding models for the integrated expansion of generation and transmission facilities based on mixed-integer linear programming (MILP) models.

In this paper, we propose a stochastic programming model that includes relevant features for a region with very high solar irradiation that aims at the transition to a power system based on solar and wind power. A two-stage decision framework that enables investment decisions at the first stage and operation decisions at the second stage. The uncertainty characterization includes long- and short-term uncertainties to capture demand growth, but also the uncertain output of weather dependent sources. The generation technologies include solar power plants (photovoltaic (PV) and concentrated solar), wind farms, energy storage, and flexible combined cycle gas turbines. Energy storage is considered as a component of concentrated solar power (CSP) plants, but also as independent plants.

Considering the literature review above, the contribution

of this paper are threefold.

1) A generation and transmission expansion planning model is developed for power systems of regions with very high and stable solar irradiation. We illustrate such model through a comprehensive study pertaining the particular case of Saudi Arabia.

2) A number of case studies are analyzed in which increasing levels of renewable penetration are imposed in advance. Since we consider regions with very high and stable solar irradiation, very high integration of solar resources is a natural choice. We analyze the economic and technical consequences of such integration levels.

3) Policy observations are derived from our analysis and case study, which are generally applicable to power systems of regions with very high and stable solar irradiation.

The rest of this paper is organized as follows. Section II describes the formulation of the proposed generation and transmission expansion planning model. Section III applies this model to the Saudi Arabian power system and analyzes the outcomes obtained. Finally, Section IV provides conclusions and recommendations.

II. FORMULATION

The proposed model has the form as follows.

$$\min \left[\sum_{l \in \Omega^L} I_l^N x_l + \sum_{s \in \Omega^S} I_s^S P_s^{S,\max} + \sum_{w \in \Omega^W} I_w^W P_w^{W,\max} + \sum_{j \in \Omega^J} I_j^J P_j^{J,\max} + \sum_{b \in \Omega^B} I_b^B E_b^{B,\max} + \sum_{\delta} \beta_{\delta} \sum_o \alpha_o \sum_{t=1}^{24} \left(\sum_{j \in \Omega^J} C_j^J p_{\delta,j,o,t}^J + \sum_{s \in \Omega^S} C_s^S F_{\delta,s,t,o}^S P_s^{S,\max} + \sum_{w \in \Omega^W} C_w^W F_{\delta,w,t,o}^W P_w^{W,\max} + \sum_{d \in \Omega^D} C_d^{D,U} P_{\delta,d,o,t}^{D,U} \right) \right] \quad (1)$$

s.t.

$$0 \leq P_j^{J,\max} \leq \bar{P}_j^{J,\max} \quad \forall j \quad (2)$$

$$0 \leq P_s^{S,\max} \leq \bar{P}_s^{S,\max} \quad \forall s \quad (3)$$

$$0 \leq P_w^{W,\max} \leq \bar{P}_w^{W,\max} \quad \forall w \quad (4)$$

$$0 \leq E_b^{B,\max} \leq \bar{E}_b^{B,\max} \quad \forall b \quad (5)$$

$$\sum_{j \in \Omega^J} I_j^J P_j^{J,\max} + \sum_{s \in \Omega^S} I_s^S P_s^{S,\max} + \sum_{w \in \Omega^W} I_w^W P_w^{W,\max} + \sum_{b \in \Omega^B} I_b^B E_b^{B,\max} \leq I^G, \max \quad (6)$$

$$\sum_{l \in \Omega^L} I_l^N x_l \leq I^L, \max \quad (7)$$

$$\sigma_j x_{\delta,j,o,t} \leq p_{\delta,j,o,t}^J \leq x_{\delta,j,o,t} \quad \forall j, \forall o, \forall t, \forall \delta \quad (8)$$

$$x_{\delta,j,o,t} = P_j^{J,\max} - z_{\delta,j,o,t} \quad \forall j, \forall o, \forall t, \forall \delta \quad (9)$$

$$0 \leq x_{\delta,j,o,t} \leq \bar{P}_j^{J,\max} y_{\delta,j,o,t} \quad \forall j, \forall o, \forall t, \forall \delta \quad (10)$$

$$0 \leq z_{\delta,j,o,t} \leq \bar{P}_j^{J,\max} (1 - y_{\delta,j,o,t}) \quad \forall j, \forall o, \forall t, \forall \delta \quad (11)$$

$$p_{\delta,j,o,t}^J - p_{\delta,j,o,t-1}^J \leq R_j^U \quad \forall j, \forall o, \forall t, \forall \delta \quad (12)$$

$$p_{\delta,j,o,t-1}^J - p_{\delta,j,o,t}^J \leq R_j^D \quad \forall j, \forall o, \forall t, \forall \delta \quad (13)$$

$$0 \leq p_{\delta,d,o,t}^{D,U} \leq P_{\delta,d,t,o}^D \quad \forall d, \forall o, \forall t, \forall \delta \quad (14)$$

$$E_{\delta,b,o,t+1}^B = E_{\delta,b,o,t}^B + p_{\delta,b,o,t}^{B,P} \eta_b - p_{\delta,b,o,t}^{B,T} \quad \forall b, \forall o, \forall t, \forall \delta \quad (15)$$

$$0 \leq p_{\delta,b,o,t}^{B,T} \leq p_b^{BT,\max} \quad \forall b, \forall o, \forall t, \forall \delta \quad (16)$$

$$0 \leq p_{\delta,b,o,t}^{B,P} \leq p_b^{BP,\max} \quad \forall b, \forall o, \forall t, \forall \delta \quad (17)$$

$$0 \leq E_{\delta,b,o,t}^B \leq E_b^{B,\max} \quad \forall b, \forall o, \forall t, \forall \delta \quad (18)$$

$$F_{\delta,l,o,t}^L = B_l(\theta_{\delta,s(l),o,t} - \theta_{\delta,r(l),o,t}) \quad \forall l, l \notin \Omega^L, \forall o, \forall t, \forall \delta \quad (19)$$

$$-F_l^{L,\max} \leq F_{\delta,l,o,t}^L \leq F_l^{L,\max} \quad \forall l, l \notin \Omega^L, \forall o, \forall t, \forall \delta \quad (20)$$

$$-x_l F_l^{L,\max} \leq F_{\delta,l,o,t}^L \leq x_l F_l^{L,\max} \quad \forall l, l \in \Omega^L, \forall o, \forall t, \forall \delta \quad (21)$$

$$-(1-x_l)M \leq F_{\delta,l,o,t}^L - B_l(\theta_{\delta,s(l),o,t} - \theta_{\delta,r(l),o,t}) \leq (1-x_l)M \quad \forall l, l \in \Omega^L, \forall o, \forall t, \forall \delta \quad (22)$$

$$\begin{aligned} & \sum_{j \in \Omega_n^J} P_{\delta,j,o,t}^J + \sum_{s \in \Omega_n^S} F_{\delta,s,t,o}^S P_s^{S,\max} - \sum_{s \in \Omega_n^S} P_{\delta,s,t,o}^{S,spill} + \sum_{w \in \Omega_n^W} F_{\delta,w,t,o}^W P_w^{W,\max} - \\ & \sum_{w \in \Omega_n^W} P_{\delta,w,t,o}^{W,spill} + \sum_{b \in \Omega_n^B} P_{\delta,b,o,t}^{BT} - \sum_{l|s(l)=n} F_{\delta,l,o,t}^L + \sum_{l|r(l)=n} F_{\delta,l,o,t}^L = \\ & \sum_{d \in \Omega_n^D} (P_{\delta,d,t,o}^D - P_{\delta,d,o,t}^{D,U}) + \sum_{b \in \Omega_n^B} P_{\delta,b,o,t}^{BP} \quad \forall n, \forall o, \forall t, \forall \delta \end{aligned} \quad (23)$$

$$\begin{aligned} & \varphi^{EE} \left[\sum_o \alpha_o \sum_{t=1}^{24} \left(\sum_{s \in \Omega_n^S} F_{\delta,s,t,o}^S P_s^{S,\max} + \sum_{w \in \Omega_n^W} F_{\delta,w,t,o}^W P_w^{W,\max} + \sum_{j \in \Omega_n^J} P_{\delta,j,o,t}^J \right) \right] \leq \\ & \sum_o \alpha_o \sum_{t=1}^{24} \left(\sum_{s \in \Omega_n^S} F_{\delta,s,t,o}^S P_s^{S,\max} + \sum_{w \in \Omega_n^W} F_{\delta,w,t,o}^W P_w^{W,\max} \right) \quad \forall \delta \end{aligned} \quad (24)$$

$$\varphi^C \left(\sum_{j \in \Omega^J} P_j^{J,\max} + \sum_{s \in \Omega^S} P_s^{S,\max} + \sum_{w \in \Omega^W} P_w^{W,\max} \right) \leq \sum_{s \in \Omega^S} P_s^{S,\max} + \sum_{w \in \Omega^W} P_w^{W,\max} \quad (25)$$

$$\begin{aligned} & \varphi^{EA} \left[\sum_{\delta} \beta_{\delta} \sum_o \alpha_o \left(\sum_{s \in \Omega_n^S} F_{\delta,s,t,o}^S P_s^{S,\max} + \sum_{w \in \Omega_n^W} F_{\delta,w,t,o}^W P_w^{W,\max} + \sum_{j \in \Omega_n^J} P_{\delta,j,o,t}^J \right) \right] \leq \\ & \sum_{\delta} \beta_{\delta} \sum_o \alpha_o \sum_{t=1}^{24} \left(\sum_{s \in \Omega_n^S} F_{\delta,s,t,o}^S P_s^{S,\max} + \sum_{w \in \Omega_n^W} F_{\delta,w,t,o}^W P_w^{W,\max} \right) \end{aligned} \quad (26)$$

$$-\pi \leq \theta_{\delta,n,o,t} \leq \pi \quad \forall n, \forall o, \forall t, \forall \delta \quad (27)$$

$$\theta_{\delta,n,o,t} = 0 \quad n \in \Omega_r, \forall o, \forall t, \forall \delta \quad (28)$$

$$y_{\delta,j,o,t} \in \{0, 1\} \quad \forall j, \forall o, \forall t, \forall \delta \quad (29)$$

$$x_l \in \{0, 1\} \quad \forall l \in \Omega^L \quad (30)$$

where $\Delta = \{P_{\delta,j,o,t}^J, F_{\delta,l,o,t}^L, P_{\delta,d,o,t}^{D,U}, P_j^{J,\max}, P_s^{S,\max}, P_w^{W,\max}, P_{\delta,w,t,o}^{W,spill}, P_{\delta,s,t,o}^{S,spill}, P_{\delta,b,o,t}^{B,P}, P_{\delta,b,o,t}^{B,T}, E_b^{B,\max}, E_{\delta,b,o,t}^B, y_{\delta,j,o,t}, x_{\delta,j,o,t}, z_{\delta,j,o,t}, x_l, \theta_{\delta,n,o,t}\}$.

The terms included in objective function (1) are as follows.

1) $\sum_{l \in \Omega^L} I_l^N x_l$ is the annualized investment cost of new transmission lines.

2) $\sum_{s \in \Omega^S} I_s^S P_s^{S,\max}$ is the annualized investment cost of new solar units.

3) $\sum_{w \in \Omega^W} I_w^W P_w^{W,\max}$ is the annualized investment cost of new wind units.

4) $\sum_{j \in \Omega^J} I_j^J P_j^{J,\max}$ is the annualized investment cost of new combined cycle gas turbines (CCGTs).

5) $\sum_{b \in \Omega^B} I_b^B E_b^{B,\max}$ is the annualized investment cost of new storage units.

6) $\sum_{j \in \Omega^J} C_j^J P_{\delta,j,o,t}^J + \sum_{s \in \Omega^S} C_s^S F_{\delta,s,t,o}^S P_s^{S,\max} + \sum_{w \in \Omega^W} C_w^W F_{\delta,w,t,o}^W P_w^{W,\max}$, $\forall o, \forall t, \forall \delta$ is the operation cost of all units.

7) $\sum_{d \in \Omega^D} C_d^{D,U} P_{\delta,d,o,t}^{D,U}$, $\forall o, \forall t, \forall \delta$ is the load-shedding cost.

Both terms 6 and 7 are multiplied by the weight of the day type α_o and the weight of the corresponding scenario β_{δ} .

Constraints (2)-(7) are investment constraints. Among them, constraints (2)-(4) impose bounds on the production capacity of each generation unit to be built. Likewise, constraint (5) imposes bounds on the storage energy capacity of each storage unit to be built. Constraints (6) and (7) specify the investment budgets for building new generation units (all technologies) and new transmission lines, respectively.

Constraints (8)-(29) are operation constraints. Among them, the sets of mixed-integer linear constraints (8)-(11) replace the nonlinear constraint $\sigma_j P_j^{J,\max} y_{\delta,j,o,t} \leq p_{\delta,j,o,t} \leq P_j^{J,\max} y_{\delta,j,o,t}$. This constraint imposes power output bounds on any new CCGT. Constraints (12) and (13) define the ramping-up and ramping-down limits of CCGT. Constraint (14) bounds the load-shedding of demand. Constraints (15)-(18) impose charging and discharging limits for each storage unit. Constraint (19) gives the power flow through the existing transmission line. Constraint (22) is the linearization of the nonlinear constraint $F_{\delta,l,o,t}^L = x_l B_l(\theta_{\delta,s(l),o,t} - \theta_{\delta,r(l),o,t})$. This constraint gives the power flow through the prospective transmission line. Constraints (20) and (21) limit the power flows through any transmission line. Constraint (23) enforces the power balance at each node. Constraint (24) enforces a minimum level of renewable energy per scenario. Constraint (25) enforces a minimum level of renewable power. Constraint (26) enforces a minimum level of average renewable energy. Constraint (27) establishes bounds for voltage angles at each node. Constraint (28) sets the voltage angle to be 0 at the reference node n . Constraint (29) defines binary variable $y_{\delta,j,o,t}$, $\forall o, \forall t, \forall \delta$. Finally, constraint (30) defines binary variable x_l .

Overall, the proposed stochastic programming model is translated into a large-scale MILP problem that can be solved using commercially available solvers. Binary variables pertain to both investment decisions in transmission lines and unit commitment decisions for CCGTs. Note that binary variables to avoid the simultaneous charging and discharging of energy storage are not incorporated. Capacity additions are modelled as continuous variables. This constitutes a reasonable trade-off between modelling accuracy and computation tractability.

III. CASE STUDY OF SAUDI ARABIAN POWER SYSTEM

In this section, we apply the proposed generation and transmission expansion planning model to the Saudi Arabian power system. This case study corresponds to a realistic description of the Saudi Arabian power system. Saudi Arabia benefits from very high solar irradiation and plans to introduce renewable sources in its generation mix, as defined in the Governmental Plan Vision 2030 [17]. Besides this energy transition plan, the Saudi Arabian government has al-

ready started the building process of a new city, NEOM, that will be run on 100% renewable energy [18]. At a regional scale, the potential of solar power in Saudi Arabia is assessed in [19]. The cost of including PV technology in the Saudi Arabian power system is studied in [20], where the KAPSARC energy model is extended to include solar PV. They perform several cost and benefit analyses considering a maximum installation of 20 GW capacity of solar PV. Reference [21] analyzes the benefits of energy and water storage

in a future 100% renewable energy power system in Saudi Arabia. Reference [22] gives an overview of renewable energy in Saudi Arabia and analyzes the potential of renewable energy in that country.

A. Data

The generation and load data of the Saudi Arabian power system are obtained from [19], whereas the data of locations and transmission lines can be found in [23]. Figure 1 depicts a simplified version of Saudi Arabian 380 kV power system.

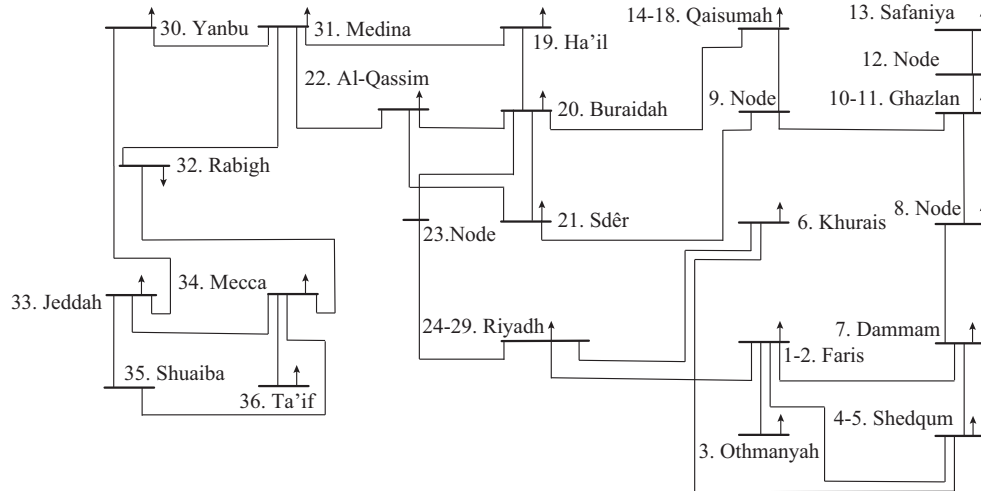


Fig. 1. Schematic diagram of simplified version of Saudi Arabian 380 kV power system.

Renewable energy data for Saudi Arabia are obtained from the system advisor model (SAM) [24], and weather data for Saudi Arabia are obtained from the PV geographical information system website [25]. In addition, investment cost data for all generation units are obtained from National Renewable Energy Laboratory (NREL) website [26]. The operation costs for renewable technologies are obtained from the USA Energy Information Administration (EIA) website [27] except for CSP units, which are obtained from the SAM [24].

We apply the capital recovery factor $r(1+r)^x / [(1+r)^x - 1]$ to the investment cost data to compute the annualized investment, where r is the real interest rate, and x is the number of years for the depreciation period. We annualize the investment costs by assuming a 25-year depreciation period and a 9% real interest rate. This yields an 10% cost-annualization rate.

We use a greenfield approach with respect to generation facilities, but not with respect to transmission lines. The target planning year is 2040. Due to unattractive wind profiles across the Arabian peninsula, only 9 locations are selected as candidates for installing onshore wind power plants. These locations correspond to nodes 7, 6, 13, 23, 24, 30, 31, 32, and 33. The annualized investment cost of any onshore wind unit is 172200 \$/MW and its operation cost is 2.8 \$/MWh. We consider that it is possible to build up to 22 PV power plants, and up to 22 CSP power plants. The annualized investment cost of any PV power plant is 106900 \$/MW and its operation cost is 2.5 \$/MWh. PV power plants can be located at any node except nodes 9 and 12. The annualized investment cost of any CSP power plant is 371000 \$/MW and its operation cost is 4.7 \$/MWh. We assume that each CSP

power plant has a thermal energy storage (TES) system with 12 hours of energy storage capacity. CSP power plants can be located at any node except nodes 9 and 12.

Regarding storage units, we consider compressed air energy storage (CAES) with an annualized investment cost of 48000 \$/MW [28]. The energy efficiency is assumed to be 0.7 p.u. and the energy capacity is considered to be 10 hours times the power capacity. Different types of storage technologies characterized by different investment costs and efficiencies can be represented in the proposed model. Storage units can be located at any node except nodes 9 and 12.

We consider the possibility of installing CCGTs, whose investment cost is 89500 \$/MW and the variable cost is 35 \$/MWh. CCGTs can be located at any node except nodes 9 and 12. Table I provides the characteristics of existing transmission lines including their capacities and Table II provides the characteristics of 12 prospective lines including their capacities as well. The annualized investment cost of AC transmission lines is assumed to be 24000 \$/km.

B. Scenarios and Representative Days

The electric power demand during the day and night is flat in Saudi Arabia, both during the winter and summer. A representative demand curve can be observed in Fig. 2. The demand is flat because its most important component is air conditioning, and since ambient temperature does not change significantly from day to night, the need for air conditioning remains rather stable. The demand level in the summer is higher than that in the winter, but both are rather flat. Under these conditions, a few days are sufficient to accurately represent the whole year.

TABLE I
TECHNICAL CHARACTERISTICS OF EXISTING TRANSMISSION LINES

l	Corridor	Length (km)	Capacity (MW)	l	Corridor	Length (km)	Capacity (MW)
1	7-2	100	1610	17	20-21	186	1000
2	7-5	50	1610	18	20-22	127	1500
3	2-24	356	400	19	20-23	250	700
4	2-5	75	1610	20	22-31	480	600
5	5-6	150	1310	21	23-24	100	1300
6	6-24	180	700	22	31-30	270	700
7	7-8	41	1610	23	30-32	162	1300
8	8-10	20	1610	24	31-32	320	700
9	9-10	75	1450	25	21-22	100	800
10	9-14	100	1610	26	32-33	170	850
11	9-21	421	500	27	32-34	178	800
12	10-12	180	1260	28	33-34	70	1610
13	12-13	20	1000	29	33-35	52	1200
14	14-20	406	700	30	34-36	76	1610
15	19-31	400	700	31	34-35	80	800
16	19-20	274	700				

TABLE II
TECHNICAL CHARACTERISTICS OF PROSPECTIVE TRANSMISSION LINES

l	Corridor	Length (km)	Capacity (MW)	Annualized investment cost (10^3 \$)
32	7-8	41	1610	984
33	2-8	140	800	3360
34	2-10	160	1610	3840
35	32-33	170	900	4080
36	33-36	80	1610	1920
37	34-35	80	800	1920
38	32-34	178	900	4272
39	24-19	624	400	14976
40	31-32	320	600	7680
41	8-10	20	1610	480
42	33-35	52	1100	1248
43	2-24	356	700	8544

The current peak demand of the Saudi Arabian power system is 49 GW [23]. Regarding long-term uncertainty and based on historical trends, we consider three different future load scenarios. The weights of these three scenarios are 1.1, 1.3, and 1.5, respectively, and their probabilities are 0.2, 0.3, and 0.5, respectively ($\sum \beta_s = 1$). Econometric models could be used to estimate such potential growths and their probabilities, which is outside the scope of our work. Needless to say, additional scenarios including extreme low-probability ones can be incorporated at the cost of increasing the computation burden of the proposed model.

Based on historical data, we use eight typical days to represent the target year (2040). We use two typical days (spanning 24 hours) for each season of the year. The weight of each representative day is the number of days in the corresponding season ($\sum \alpha_o = 365$). Note that it is a good enough

approximation as most days in a given season in Saudi Arabia are virtually identical in term of demand, wind- and solar-production patterns. This is also the most likely outcome of a k -means algorithm to cluster days.

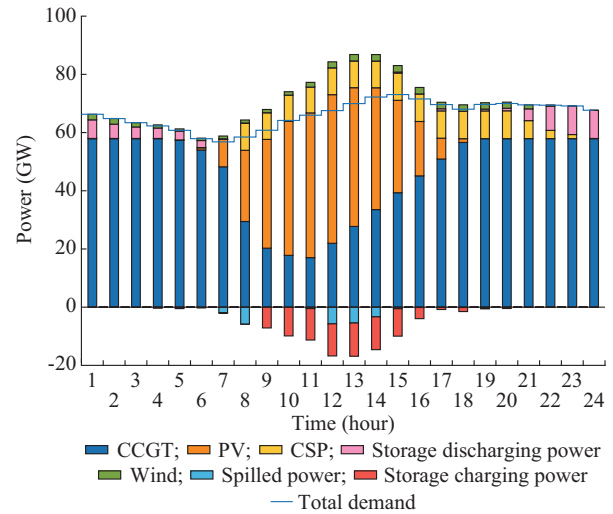


Fig. 2. Unit commitment decisions in the worst case scenario in case 3 with $X = 60$.

C. Case Studies

Planning target refers to a future outcome objective, e.g., achieving at least 80% renewable energy production in 2040. The scenario refers to a realization of the future peak load (long-term uncertain parameter), e.g., 20% above the forecasting value. We consider four case studies, which are characterized as follows.

1) BAU: in this case, there are no restrictions in building CCGTs.

2) $X\%$ renewable energy per scenario: in this case, up to $100\% - X\%$ of the total energy per scenario can be produced using thermal units ($\varphi^{EE} = X/100$ in (24)).

3) $X\%$ renewable power: in this case, only $100\% - X\%$ of the total power capacity built can be thermal ($\varphi^C = X/100$ in (25)).

4) $X\%$ average renewable energy for the three scenarios: in this case, up to $100\% - X\%$ of the total average energy for the three scenarios can be produced using thermal units ($\varphi^{EA} = X/100$ in (26)).

We pay particular attention below to case 2 due to its practical relevance.

To solve these cases, we use CPLEX [29] under GAMS [30] on a Windows PC with an Intel Core i5/2.4 GHz processor and 8 GB of RAM. The computation time required is approximately 48 hours for each case. An instance of this model includes 4047 binary variables, 126064 continuous variables, and 193347 equations. The solution is obtained within a relative optimality gap below 0.001%. Analyzing very large systems, e.g., the China southern power grid or the power system of the East Coast of the USA, would require using powerful computers (not a personal computer), but the modelling framework would remain unchanged.

D. Results

1) Case Comparison

The investment, operation, and total costs for cases 1 and 2 are shown in Table III and for cases 3 and 4 are shown in Table IV, where Δ_1 , Δ_2 , Δ_3 are the increments of the investment cost, operation cost and total cost with respect to BAU, respectively. Results for cases 1 and 2 of total capacity to be built for each technology are given in Table V and for cases 3 and 4 are given in Table VI. It can be observed that if thermal limits are imposed, PV increases significantly due to its comparatively low investment cost. Although the energy efficiency of a CSP power plant is higher than that of a PV or wind power plant, the high capital cost of CSP makes this technology comparatively unattractive. As expected, the wind capacity built is low since wind conditions are not attractive. The capacity of energy storage units increases with the renewable capacity to store the energy from solar power plants to meet the demand during the night.

TABLE III
INVESTMENT, OPERATION, AND TOTAL COSTS FOR CASES 1 AND 2

Case	X	Investment cost (10^{10} \$)	Δ_1 (%)	Operation cost (10^{10} \$)	Δ_2 (%)	Total cost (10^{10} \$)	Δ_3 (%)
1		1.0190		1.4000		2.4190	
	30	1.4491	42	1.2464	-11	2.6955	11
	40	2.0174	98	1.0801	-23	3.0975	28
	50	2.4708	142	0.9544	-32	3.4252	41
2	60	2.8807	183	0.7341	-48	3.6148	49
	70	3.6902	262	0.6047	-57	4.2949	77
	80	4.5250	344	0.4756	-66	5.0006	106
	90	6.3954	528	0.2926	-79	6.6880	176
	100	7.6509	651	0.1600	-89	7.8109	222

TABLE IV
INVESTMENT, OPERATION, AND TOTAL COSTS FOR CASES 3 AND 4

Case	X	Investment cost (10^{10} \$)	Δ_1 (%)	Operation cost (10^9 \$)	Δ_2 (%)	Total cost (10^{10} \$)	Δ_3 (%)
3	60	1.8562	82	9.169	-35	2.7732	14
4	60	2.6520	160	6.669	-52	3.3189	37
3	80	3.5324	247	5.877	-58	4.1201	70
4	80	4.0220	295	4.119	-71	4.4339	83

TABLE V
CAPACITY OF EACH TECHNOLOGY BUILT FOR CASES 1 AND 2

Case	X	Capacity (MW)					Total
		CCGT	PV	CSP	Wind	Energy storage	
1		66280	10770	3012	0	8840	88902
	30	65968	20939	8386	4275	11120	110688
	40	64282	54249	13610	5980	11300	149421
	50	61787	64525	18802	14350	12598	172062
	60	57195	74895	28200	13300	13022	186612
2	70	46020	95660	34402	11200	34960	222242
	80	34840	116400	40826	10064	56933	259063
	90	12480	157860	73628	6625	77804	328397
	100	0	201413	67774	2947	130341	402476

TABLE VI
CAPACITY OF EACH TECHNOLOGY BUILT FOR CASES 3 AND 4

Case	X	Capacity (MW)					Total
		CCGT	PV	CSP	Wind	Energy storage	
3	60	60109	82794	5160	2210	9055	159328
4	60	57353	71290	23425	13538	12200	177806
3	80	42613	166091	922	3439	56982	270047
4	80	40400	98155	38037	12210	43990	232792

In case 1, the renewable power capacity is just 17% of the total power capacity. The total cost of case 1 is the lowest, and the highest total cost is that of the 100% renewable case. Since thermal units have the lowest investment cost and the highest operation cost, the operation cost of case 1 is the highest and the investment cost is the lowest.

Besides case 1, we observe that imposing a requirement based on renewable energy per scenario is the most expensive option. The lowest cost option is imposing a requirement based on renewable capacity.

Figure 3 shows the investment, operation, and total costs as a function of the renewable power built for cases 1 and 2 with X ranging from 30 to 100. The total cost increases significantly beyond $X = 80$.

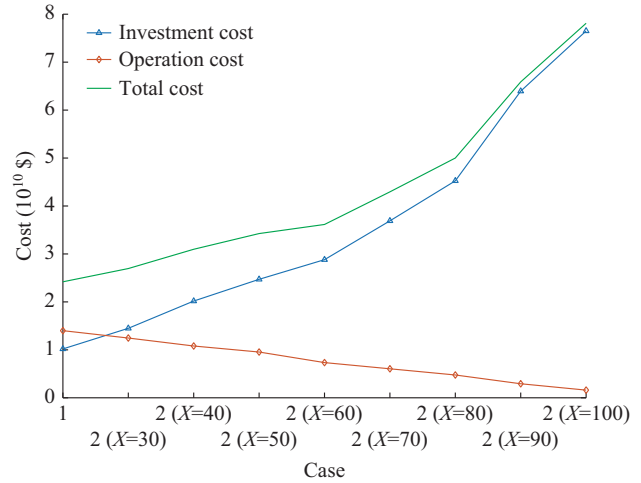


Fig. 3. Investment, operation, and total costs as a function of renewable power.

Based on these results, it can be concluded that case 2 with $X = 60$ is a competitive option. Indeed, it is possible to increase the percentage of renewable energy per scenario from 17% (BAU) to 60% with an increment in total cost of 49% with respect to BAU.

The case 3 with $X = 60$ is a good compromise between cost and renewable integration over all options. It achieves comparatively low operation cost and results in 43% shift in total renewable energy with 14% increment in total cost with respect to BAU. The case 4 with $X = 80$ achieves a high level of renewable penetration, but at a comparatively high cost. However, it is a much more attractive option in terms of cost than case 2 with $X = 80$. Exceeding $X = 80$ in case 2 requires high investment cost and the system would

have a large amount of lightly used capacity.

2) Representative Days

The demand throughout the hours of the day at different locations and the renewable production throughout the day at different production locations are “short-term” uncertain parameters that we model using 8 representative days. To assess the stability of the results, we have also run case 1 with 12 representative days. Note that in Saudi Arabia, the demand and the renewable production are rather stable throughout the winter and summer (the only seasons in this country). Table VII shows that the results of case 1 for 8 and 12 representative days have the similar renewable penetration levels and investment costs. The operation costs decrease as a result of incorporating less extreme operation conditions. Therefore, only a few representative days are required to accurately represent the whole year.

3) Worst Operation Condition (Day) in Case 3 with $X = 60$

The worst operation condition (day) in case 3 with $X = 60$ corresponds to day 3 and scenario 3 (peak demand of 73 GW).

TABLE VII
COSTS OF CASE 1 FOR 8 AND 12 REPRESENTATIVE DAYS

Time (day)	Investment cost (10^{10} \$)	Operation cost (10^{10} \$)	Total cost (10^{10} \$)	Renewable penetration level (%)
8	1.019	1.40	2.42	17
12	1.018	1.36	2.38	17

Figure 4 shows the newly built generator and transmission facilities in case 3 with $X = 60$. Figure 2 depicts the hourly production of each technology to supply the demand. It can be observed that wind units do not produce power during the night when PV and CSP units cannot produce power, which forces the system to use thermal units with high ramping capabilities. Otherwise, the model results would include building additional solar units to cover daytime demand. It can be observed that the energy storage units help the system use solar energy more efficiently. Indeed, they allow the system to use 59 GWh of solar energy during the night.

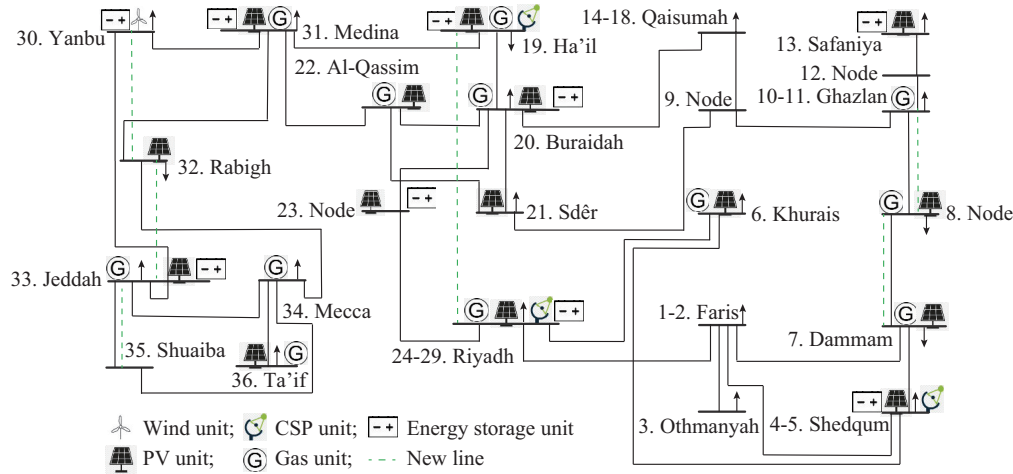


Fig. 4. Newly built generator and transmission facilities in case 3 with $X = 60$.

4) Results of Transmission Line

Table VIII provides the number of transmission lines built in each case. Case 1 includes the lowest number of transmission lines built, where the highest corresponds to case 2 with $X = 80$. If we consider the Saudi Arabian power system has no existing transmission lines, the number of the transmission lines built in case 3 with $X = 60$ will be smaller than that in case 1.

TABLE VIII
NUMBER OF TRANSMISSION LINES BUILT

Case	X	No. of transmission lines	Case	X	No. of transmission lines
1		2	2	80	12
2	60	9	3	80	9
3	60	6	4	80	11
4	60	9			

E. Cost Projections

EIA [27] provides three future pathways of capacity cost

for different types of power plants. Approximately, the low and medium pathways have very similar cost assumptions, but the high pathway has significantly higher cost assumptions.

1) High Cost Assumption

We analyze how the investment and operation costs change as a function of a high pathway cost assumption. Figure 5 shows the increase in investment and operation costs with respect to medium pathway assumption.

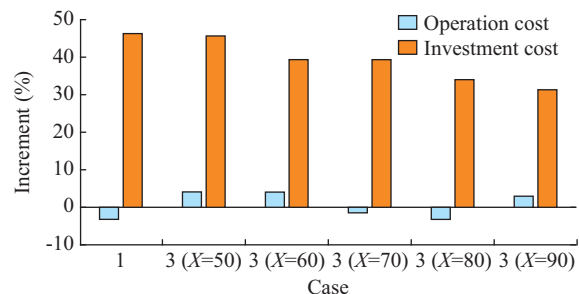


Fig. 5. Increment in investment and operation costs of high pathway assumption with respect to medium pathway assumption.

The cases considered include case 1 and case 3 with X ranging from 50 to 90. It can be observed that the increment in investment costs decrease as the renewable capacity increases. This is because the investment cost of case 1 is the smallest and increases as the renewable penetration level increases, as shown in Fig. 3.

2) Only PV Investment Cost is High

In the previous cases, PV dominated the renewable energy due to its low investment cost. Thus, we analyze the result if only PV investment costs are comparatively high and other technologies remain at the medium pathway assumption. Figure 6 shows the increment in investment and operation costs with respect to medium pathway assumption when only PV investment costs are comparatively high. The cases considered include case 1 and case 3 with X ranging from 50 to 90.

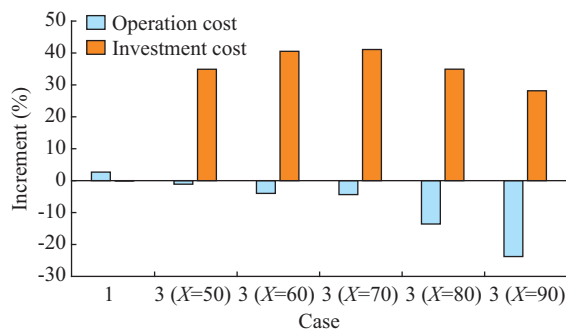


Fig. 6. Increment in investment and operation costs with respect to medium pathway assumption when only PV investment costs are comparatively high.

Figure 7 illustrates the difference of renewable and CCGT power built with respect to medium pathway assumption when only PV investment costs are comparatively high.

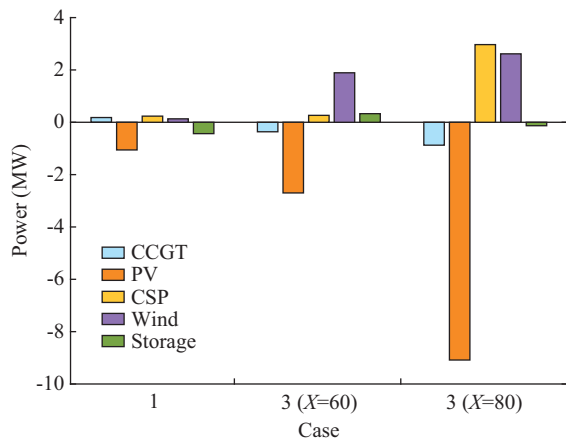


Fig. 7. Difference of renewable and CCGT power built with respect to medium pathway assumption when only PV investment costs are comparatively high.

Comparing the results, it can be observed that the renewable power capacity built in case 1 decreases from 17% to 10% of the total power capacity if we change the investment cost of PV technology from medium to high pathway assumption.

IV. CONCLUSION

This paper uses a long-term generation and transmission planning model to analyze the transition of the Saudi Arabian power system toward high penetration level of renewable sources. Considering the case studies carried out, the conclusions are drawn as follow.

1) Regarding a renewable penetration level of only 17% in case 1, we can conclude that it is important to actively promote the integration of renewable power in the Saudi Arabian power system if a high penetration level of renewable sources is desired.

2) Since a high renewable penetration level is achieved using PV and CSP, which do not operate during the night, high generation and storage capacities need to be installed. This is specific to Saudi Arabia since attractive wind sites are not available.

3) Our model and analyses are applicable to power systems in geographical areas with high solar irradiation and stable weather condition.

An out-of-sample analysis for assessing the comparative performance of alternative expansion plans is a fruitful area of additional research.

REFERENCES

- [1] P. Sullivan, K. Eurek, and R. Margolis, "Advanced methods for incorporating solar energy technologies into electric sector capacity-expansion models: literature review and analysis," National Renewable Energy Laboratory (NREL), Golden, USA, Tech. Rep. NREL/TP-6A20-61185, 2014.
- [2] O. M. Babatunde, J. L. Munda, and Y. Hamam, "A comprehensive state-of-the-art survey on power generation expansion planning with intermittent renewable energy source and energy storage," *International Journal of Energy Research*, vol. 43, no. 4, pp. 6078-6107, Mar. 2019.
- [3] A. S. Dagoumas and N. E. Koltsaklis, "Review of models for integrating renewable energy in the generation expansion planning," *Applied Energy*, vol. 242, pp. 1573-1587, May 2019.
- [4] H. Sadeghi, M. Rashidinejad, and A. Abdollahi, "A comprehensive sequential review study through the generation expansion planning," *Renewable and Sustainable Energy Reviews*, vol. 67, pp. 1369-1394, Jan. 2017.
- [5] L. Baringo and A. Conejo, "Transmission and wind power investment," *IEEE Transactions on Power Systems*, vol. 27, no. 2, pp. 885-893, May 2012.
- [6] P. Denholm, "Energy storage to reduce renewable energy curtailment," in *Proceedings of IEEE PES General Meeting*, San Diego, USA, Jul. 2012, pp. 1-4.
- [7] M. Hand, S. Baldwin, E. Demeo *et al.* (2012, Jun.). Renewable electricity futures study. [Online]. Available: <http://www.nrel.gov>
- [8] J. Aghaei, N. Amjadi, A. Baharvandi *et al.*, "Generation and transmission expansion planning: MILP-based probabilistic model," *IEEE Transactions on Power Systems*, vol. 29, no. 4, pp. 1592-1601, Jul. 2014.
- [9] H. Park and R. Baldick, "Stochastic generation capacity expansion planning reducing greenhouse gas emissions," *IEEE Transactions on Power Systems*, vol. 30, no. 2, pp. 1026-1034, Mar. 2015.
- [10] N. van Bracht, F. Grote, A. Fehler *et al.*, "Incorporating long-term uncertainties in generation expansion planning," in *Proceedings of 2016 13th International Conference on the European Energy Market*, Porto, Portugal, Jun. 2016, pp. 1-10.
- [11] K. Poncelet, H. Hoeschle, E. Delarue *et al.*, "Selecting representative days for capturing the implications of integrating intermittent renewables in generation expansion planning problems," *IEEE Transactions on Power Systems*, vol. 32, no. 3, pp. 1936-1948, May 2017.
- [12] Y. Zhan, Q. Zheng, J. Wang *et al.*, "Generation expansion planning with large amounts of wind power via decision-dependent stochastic programming," *IEEE Transactions on Power Systems*, vol. 32, no. 4, pp. 3015-3026, Jul. 2017.
- [13] C. L. Lara, D. S. Mallapragada, D. J. Papageorgiou *et al.*, "Determinis-

- tic electric power infrastructure planning: mixed-integer programming model and nested decomposition algorithm,” *European Journal of Operational Research*, vol. 271, no. 3, pp. 1037-1054, Dec. 2018.
- [14] R. Domínguez, A. J. Conejo, and M. Carrión, “Toward fully renewable electric energy systems,” *IEEE Transactions on Power Systems*, vol. 30, no. 1, pp. 316-326, Jan. 2015.
- [15] Q. Xu, S. Li, and B. F. Hobbs, “Generation and storage expansion co-optimization with consideration of unit commitment,” in *Proceedings of 2018 IEEE International Conference on Probabilistic Methods Applied to Power Systems*, Boise, USA, Jun. 2018, pp. 1-9.
- [16] A. Conejo, L. Morales, S. Kazempour *et al.*, *Investment in Electricity Generation and Transmission: Decision Making Under Uncertainty*. New York: Springer, 2016.
- [17] Saudi Arabia Government. (2019, Jul.). Saudi vision 2030. [Online]. Available: <https://vision2030.gov.sa/en>
- [18] Saudi Arabia Government. (2019, Jun.). NEOM. [Online]. Available: <http://www.neom.com>
- [19] Saudi Electricity Company. (2019, May). SEC annual report 2015. [Online]. Available: <https://www.se.com.sa/en-us>
- [20] A. Elshurafa and W. Matar, “Adding solar PV to the saudi power system: what is the cost of intermittency?” *Energy Transitions*, vol. 1, no. 1, p. 2, Jun. 2017.
- [21] U. Caldera and C. Breyer, “The role that battery and water storage play in Saudi Arabias transition to an integrated 100% renewable energy power system,” *Journal of Energy Storage*, vol. 17, pp. 299-310, Jun. 2018.
- [22] S. El-Nakla, C. B. Yahya, H. Peterson *et al.*, “Renewable energy in Saudi Arabia: current status initiatives and challenges” in *Proceedings of 9th IEEE-GCC Conference and Exhibition*, Bahrain, The Kingdom of Bahrain, May 2017, pp. 1-10.
- [23] Electricity and Cogeneration Regulatory Authority. (2019, May). Electricity and co-generation regulatory authority. [Online]. Available: <https://www.ecra.gov.sa/en-us>
- [24] N. Blair, A. Dobos, J. Freeman *et al.* (2019, Jun.). System advisor model, SAM 2014.1.14: general description. [Online]. Available: <http://www.nrel.gov/docs/fy14osti/61019.pdf>
- [25] EU Science Hub. (2019, May). Photovoltaic geographical information system. [Online]. Available: <https://ec.europa.eu/jrc/en/scientific-tool/pvgis>
- [26] National Renewable Energy Laboratory. (2019, May). Renewable electricity futures study. [Online]. Available: <https://www.nrel.gov>
- [27] The U.S. Energy Information Administration. (2019, May). Form EIA-860. [Online]. Available: <https://www.eia.gov>
- [28] K. Zach, H. Auer, and G. Lettner. (2012, Aug.). Facilitating energy storage to allow high penetration of intermittent renewable energy. [Online]. Available: <https://www.mendeley.com/catalogue/c0ca8ac2-879a-3ace-a5ac-97026afdd6fd/>
- [29] GAMS. (2019, May). CPLEX 12. [Online]. Available: <https://www.gams.com/latest/docs>
- [30] A. Brooke, D. Kendrick, A. Meeraus *et al.* (1988, Dec.). GAMS: a user’s guide. [Online]. Available: <https://dl.acm.org/doi/10.1145/58859.58863>

Musfer Alraddadi received the M.S. degree from Western Michigan University, Kalamazoo, USA. Currently, he is a student affiliate in the Center for Operations Research, Energy, and Economics, USA and a Ph.D. candidate in the Department of Electrical and Computer Engineering at The Ohio State University, Columbus, USA. His research interests include power system planning and scheduling with high penetrations of renewable energy.

Antonio J. Conejo received the M.S. degree from the Massachusetts Institute of Technology, Cambridge, USA, in 1987, and the Ph.D. degree from the Royal Institute of Technology, Stockholm, Sweden, in 1990. He is currently a Professor in the Department of Integrated Systems Engineering and the Department of Electrical and Computer Engineering, The Ohio State University, Columbus, USA. His research interests include control, operations, planning, economics and regulation of electric energy systems as well as statistics and optimization theory and its applications.

Ricardo M. Lima received the Ph.D. degree in chemical engineering from the Faculty of Engineering, University of Porto, Porto, Portugal in 2006. He was a Post-doc Fellow and a Researcher in the Department of Chemical Engineering at the Carnegie Mellon University, Pittsburgh, USA, in 2006-2011, and an invited Researcher in PPG Industries in 2008-2011. He was a Marie Curie Fellow in the National Laboratory of Energy and Geology in Lisbon, Portugal, from 2011 to 2014. Since 2014, he is a Research Scientist in the King Abdullah University of Science and Technology, Thuwal, Saudi Arabia. His research interests include process systems engineering, energy systems, optimal path planning of autonomous underwater vehicles, and mathematical programming.